PCCP

PAPER

View Article Online
View Journal | View Issue

Open Access Article. Published on 09 marzo 2016. Downloaded on 30/09/2025 1:16:36 a.m..
This article is licensed under a Creative Commons Attribution 3.0 Unported Licence.

Cite this: *Phys. Chem. Chem. Phys.*, 2016, **18**, 9616

Investigations on HONO formation from photolysis of adsorbed HNO_3 on quartz glass surfaces

Sebastian Laufs and Jörg Kleffmann*

Received 20th January 2016,
Accepted 9th March 2016

DOI: 10.1039/c6cp00436a

www.rsc.org/pccp

During the last few decades, nitrous acid (HONO) has attracted significant attention as a major source of the OH radical, the detergent of the atmosphere. However, the different daytime sources identified in the laboratory are still the subject of controversial discussion. In the present study, one of these postulated HONO sources, the heterogeneous photolysis of nitric acid (HNO_3), was studied on quartz glass surfaces in a photo flow-reactor under atmospherically relevant conditions. In contrast to other investigations, a very low HNO_3 photolysis frequency for HONO formation of $J(HNO_3 \rightarrow HONO) = 2.4 \times 10^{-7}$ s^{-1} (0° SZA, 50% r.h.) was determined. If these results can be translated to atmospheric surfaces, HNO_3 photolysis cannot explain the significant HONO levels in the daytime atmosphere. In addition, it is demonstrated that even the small measured yields of HONO did not result from the direct photolysis of HNO_3 but rather from the consecutive heterogeneous conversion of the primary photolysis product NO_2 on the humid surfaces. The secondary NO_2 conversion was not photo-enhanced on pure quartz glass surfaces in good agreement with former studies. A photolysis frequency for the primary reaction product NO_2 of $J(HNO_3 \rightarrow NO_2) = 1.1 \times 10^{-6}$ s^{-1} has been calculated (0° SZA, 50% r.h.), which indicates that renoxification by photolysis of adsorbed HNO_3 on non-reactive surfaces is also a minor process in the atmosphere.

1. Introduction

During the last two decades, unexpectedly high nitrous acid (HONO) mixing ratios have been observed during daytime in remote,[1–5] semi urban[6–9] and urban regions.[10–17] These results stimulated laboratory investigations on potential daytime HONO sources, by (i) the reduction of nitrogen dioxide (NO_2) in the presence of organic photosensitisers,[18–21] (ii) the photolysis of adsorbed nitric acid[22–26] and (iii) bacterial production of nitrite in soil[27–30] and/or desorption of adsorbed HONO from soil surfaces during daytime.[31–33] Another intensely discussed source, the gas-phase reaction of excited NO_2 with water,[34] was found to be of minor importance as demonstrated by laboratory studies.[35,36] Also the photolysis of nitro-phenols or similar compounds is too slow to explain significant HONO levels in the daytime atmosphere.[37] Finally, a gas-phase HONO source recently postulated by Li *et al.*,[38] *i.e.* the reaction of $HO_2 \cdot H_2O$ complexes with NO_2, could not be confirmed by the same group in simulation chamber experiments[39] and is also in conflict with recent aircraft measurements.[40]

In summary, mainly ground surface sources have been identified to date in laboratory studies to explain atmospheric HONO formation during daytime,[41] which has also been confirmed by recent flux measurements in the atmosphere.[25,42,43]

Among the different proposed sources, the photolysis of adsorbed nitric acid (HNO_3) has been suggested as an important HONO formation pathway, especially in rural areas.

$$HNO_3(ads.) + h\nu \xrightarrow{J(HNO_3 \rightarrow HONO)} HONO + O, \qquad (R1)$$

Zhou and coworkers[24] have published a photolysis frequency of 1.2×10^{-5} s^{-1} for HNO_3 adsorbed on Pyrex glass, at 50% relative humidity under tropical noontime conditions, which is at least two orders of magnitude larger compared to those of liquid- and gas-phase HNO_3. In addition, the same group recently presented a correlation of HONO fluxes above a forest canopy with HNO_3 adsorbed on leaves from the surrounding trees.[25] These observations are in contrast to a smog chamber study, in which photolysis of adsorbed HNO_3 was excluded as a source of photochemical HONO formation on Teflon surfaces.[44] In these experiments significant photochemical HONO formation was still observed at wavelengths >370 nm, for which no significant light absorption of HNO_3 is expected. However, for HNO_3 adsorbed on fused silica and aluminium, a red-shift of

Physikalische und Theoretische Chemie/Fakultät für Mathematik und Naturwissenschaften, Bergische Universität Wuppertal, 42097 Wuppertal, Germany. E-mail: kleffman@uni-wuppertal.de; Fax: +49 202 439 2505; Tel: +49 202 439 3534

 This journal is © the Owner Societies 2016

Open Access Article. Published on 09 marzo 2016. Downloaded on 30/09/2025 1:16:36 a.m..
This article is licensed under a Creative Commons Attribution 3.0 Unported Licence.

the n → π* HNO_3 absorption band and more than two orders of magnitude larger UV cross-sections compared to the gas phase have been recently observed by Brewster angle cavity ring-down spectroscopy.[45–48] These observations have rekindled interest in HNO_3 as a potential HONO and NO_2 source. However, the mechanism of heterogeneous HNO_3 photolysis is still under discussion, and besides reaction (R1) secondary HONO formation pathways have also been proposed.[22,24,25,48]

To elucidate the importance of reaction (R1) as a HONO source in the atmosphere, photolysis of adsorbed HNO_3 was studied in a photo flow-reactor under atmospherically relevant concentrations, humidity and actinic flux conditions.

2. Experimental

2.1. Experimental setup

Experiments were performed in a cylindrical flow-reactor (5.0 cm i.d.) made of smooth quartz glass with an illuminated length of 56.5 cm (see Fig. 1). For a few experiments a similar flow reactor made of Pyrex glass was used. The reactor was irradiated with 6 UV-Vis lamps (Philips TL/05 40 Watt, 300–500 nm, $\lambda_{max} \approx 370$ nm; or Wolff System Helarium 40 W, 290–450 nm, $\lambda_{max} \approx 350$ nm), which were placed in an air-cooled (fan), UV-reflecting aluminium box. The actinic flux inside the photoreactor (see Fig. 2) was measured using a spectroradiometer ($\Delta\lambda = 1$ nm; Metcon Inc., USA). Calculated photolysis frequencies $J(NO_2)$ and J(HCHO) using published cross-sections and quantum yields[49–52] were compared with values directly

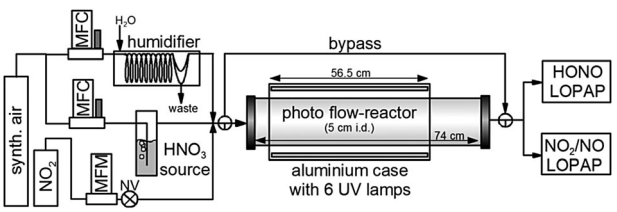

Fig. 1 Experimental setup (MFC: mass flow controller, MFM: mass flow meter, NV: needle valve).

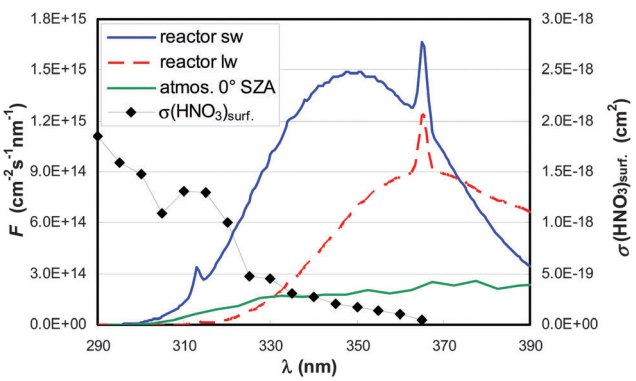

Fig. 2 Actinic flux (F) spectra of the short-(sw) and long-(lw) wavelength lamps and from the atmosphere (0° SZA).[50] The absorption spectrum σ of HNO_3 adsorbed on fused silica is also shown.[45,47]

Table 1 Calculated and measured (by chemical actinometry, in brackets) photolysis frequencies of NO_2, HONO and HCHO inside the flow-reactor for the two sets of lamps used (lw: long wavelength; sw: short wavelength). In the last column, upper limit atmospheric values (0° SZA)[54] are also listed

	lw: Philips, TL05, 40 W	sw: Wolff System, Helarium, 40 W	Atmosphere (0° SZA)
$J(NO_2)$ (s^{-1})	0.027 (0.029)	0.036	0.010
J(HONO) (s^{-1})	5.1×10^{-3}	8.7×10^{-3}	2.2×10^{-3}
$J(CH_2O)$ (s^{-1})	8.4×10^{-5}	4.8×10^{-4} (4.2×10^{-4})	8.9×10^{-5}

measured by chemical actinometry of NO_2 and HCHO in the flow-reactor and showed good agreement (see Table 1).

Corrections of the observed HONO formation for its gas-phase photolysis were typically only *ca.* 5 and 8% for the two types of lamps used, respectively. Photolysis frequencies of HONO (J(HONO), see Table 1) were calculated using published cross-sections.[53]

2.2. Instruments

HONO was measured using the sensitive LOPAP technique[10,55] with a detection limit and an accuracy of 2 pptV and 10%, respectively. NO_2 and NO were detected by a recently developed NO_2-LOPAP[56] which was modified for the additional detection of NO, details of which will be published elsewhere. In short, NO passing the NO_2 collection stripping coil was oxidized to NO_2 by an acidic $KMnO_4$ solution in a consecutive stripping coil and was detected downstream using the Griess–Saltzman reaction, similar to the NO_2 channel of the instrument. Detection limits and accuracies for NO_2/NO under the experimental conditions applied were 10/20 pptV and 7/10%, respectively. For the experimental determination of the photolysis frequency of HCHO an Aero Laser AL4001 Hantzsch instrument was used.[57] Finally, adsorbed HNO_3 was quantified by ion-chromatography (IC)[58] after elution from the flow-reactor surface with ultra-pure water (MilliPore). IC detection was also used to measure gas-phase levels of HNO_3 after bubbling through ultrapure water. The accuracy of the nitrate concentration determined by IC was 7% and those of HNO_3 in the gas phase and on the surface were 10 and 12%, respectively.

2.3. Experimental procedure

Prior to the experiments the reactor was cleaned with HF (5%) followed by ultra-pure water to minimize the contamination on the irradiated reactor surfaces. This was confirmed in blank experiments in which neither in the dark nor under irradiation any significant formation of HONO or NO_x was observed. Different reactant mixtures were generated by mixing humidified synthetic air with a pure HNO_3 gas-phase source[58] and were flushed through the flow-reactor. For some experiments low levels of NO_2 (Messer, 2 ppmV) were also added using a calibrated 10 mL min^{-1} flow meter and a needle valve. During one experiment a mixture of 29 VOCs (methane, ethane, propane, *n*-butane, iso-butane, *n*-pentane, *n*-hexane, *n*-heptane, *n*-octane, ethene, propene, iso-, *trans*-, and *cis*-butene, isoprene, β-pinene, limonene, ethine, benzene, toluene, *o*-, *m*-, and *p*-xylene, methanol, ethanol, *n*-propanol, *n*-butanol, acetone, and methacrolein) with

Open Access Article. Published on 09 marzo 2016. Downloaded on 30/09/2025 1:16:36 a.m..
This article is licensed under a Creative Commons Attribution 3.0 Unported Licence.

individual mixing ratios in the range 48–69 ppbV was added using a 100 mL min^{-1} flow controller. In some experiments additional quartz glass plates were added to the flow-reactor to increase the irradiated surface area. The total gas flow rate was typically 2.7 L min^{-1}, but was varied between 1.1 and 3.4 L min^{-1} in a few experiments leading to reaction times in the range 26–80 s.

When constant reactant concentrations were reached, the lamps were switched on and the system was analysed for photochemical HONO and NO_x formation. Immediately after each experiment and after disconnection from the HNO_3 source, the reactor was eluted with ultra-pure water and the amount of adsorbed HNO_3 was quantified. After saturation of the reactor surfaces with the continuously running HNO_3 source (typically overnight), adsorbed HNO_3 levels were assumed to be constant during each experiment. This assumption is considered plausible as the HNO_3 source produced fairly stable gas-phase levels, as demonstrated also in a former laboratory study.[58] In addition, constant gas phase HNO_3 levels at the end of the flow tube confirmed equilibrium adsorption during the experiments. This observation also indicates that the surface concentration of HNO_3 was homogeneously distributed on all the irradiated surfaces. For the calculation of surface concentrations and flux densities the geometric surface area of the flow tube was used.

3. Results and discussion

In Fig. 3, a typical experiment is shown in which adsorbed HNO_3 was irradiated without (first and last step in Fig. 3) and with different levels of added NO_2. In the absence of additional NO_2, clear positive steps in the HONO, NO and NO_2 concentrations were observed, pointing to their photochemical production.

3.1. Surface dependency

To verify whether HONO formation was caused by the photolysis of adsorbed HNO_3, reaction (R1), and not by its gas-phase photolysis,

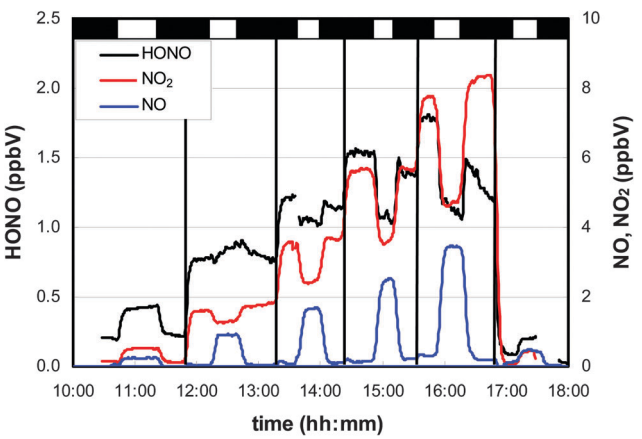

Fig. 3 HONO and NO_x formation from photolysis of adsorbed HNO_3 (7.8×10^{13} cm^{-2}) in the flow-reactor continuously flushed with humid (54% r.h.) gas-phase HNO_3. After first irradiation, NO_2 was added stepwise to the HNO_3 mixture (marked with vertical black lines). For the last step, the NO_2 addition was set to zero again. The vertical bars above the plot represent dark (black) and irradiated (white) periods.

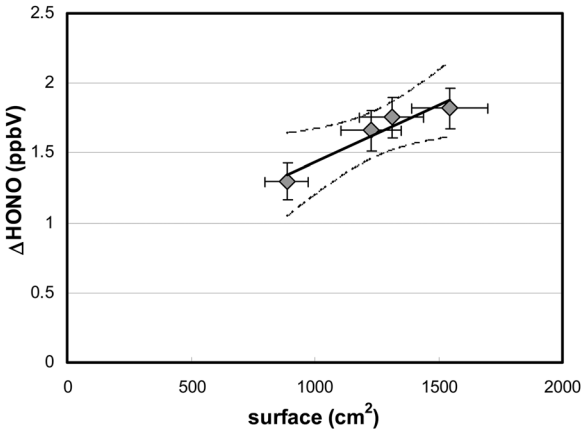

Fig. 4 HONO formation in the photolysis of adsorbed HNO_3 as a function of the reactor surface area ($[HNO_3]_{surf}$ = 1.6 × 10^{14} cm^{-2}, $[HNO_3]_g$ = 86 ppbV, 59% r.h.). The straight line represents the linear regression of the data (r^2: 0.93) with its 95% confidence limits (dashed lines).

the surface area of the reactor was varied. For these experiments, additional quartz glass plates of different sizes were added to the flow-reactor. The HONO production during irradiation increased linearly with the surface area (Fig. 4), which demonstrates the heterogeneous nature of the process involved.

This result is in agreement with theoretical calculations performed using known gas-phase absorption cross-sections of HNO_3,[51] measured actinic flux, HNO_3 gas-phase concentration, residence time in the flow-reactor and assuming an upper limit quantum yield for HONO formation of one (for calculations, see eqn (3)). The calculated maximum HONO formation by HNO_3 photolysis in the gas phase of only 6 pptV is much smaller compared to the experimental results shown in Fig. 4 and thus, a heterogeneous reaction is proposed here.

3.2. HNO_3 dependency

By varying the gas-phase concentration of HNO_3 in the range 2–120 ppbV, different quantities of surface adsorbed HNO_3 in the range 0.15–3.3 × 10^{14} molecules cm^{-2} were investigated. Recently, a surface monolayer concentration of HNO_3 of 1.1 × 10^{14} molecules cm^{-2} was estimated based on its van der Waals radius,[45] which is in fair agreement with the measured value for SiO_2 particles (7 × 10^{13} molecules cm^{-2}).[59] Thus, the investigated surface levels varied from sub-monolayer to multilayer coverage, which were obtained at atmospherically relevant low ppbV mixing ratios of the sticky HNO_3.

Photochemical HONO formation was linearly correlated with the concentration of adsorbed HNO_3, both, for the long and short wavelength lamps used (see Fig. 5). This observation is in line with a first-order surface photolysis process, reaction (R1), described by a photolysis frequency of adsorbed HNO_3 for HONO formation, $J(HNO_3 \rightarrow HONO)$, which is defined by:

$$J(\mathrm{HNO_3} \rightarrow \mathrm{HONO}) = \frac{\mathrm{d}[\mathrm{HONO}]_{\mathrm{surface}}}{\mathrm{d}t} \times \frac{1}{[\mathrm{HNO_3}]_{\mathrm{surface}}}. \quad (1)$$

Here, $\mathrm{d}[\mathrm{HONO}]_{\mathrm{surface}}/\mathrm{d}t$ represents the HONO formation rate described as a surface flux density (molecules cm^{-2} s^{-1}).

Open Access Article. Published on 09 marzo 2016. Downloaded on 30/09/2025 1:16:36 a.m..
This article is licensed under a Creative Commons Attribution 3.0 Unported Licence.

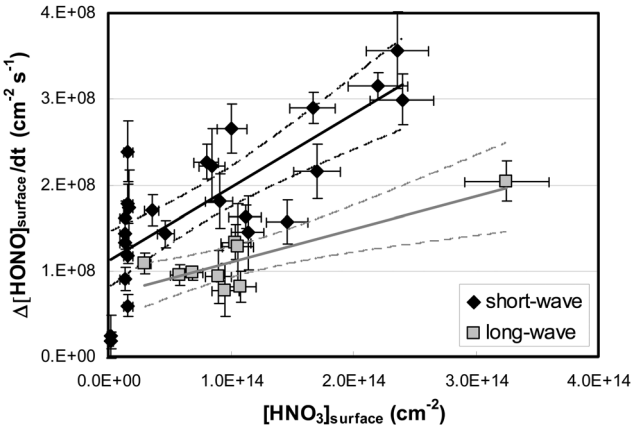

Fig. 5 HONO flux density as a function of the measured surface concentration of HNO_3 using two different sets of UV lamps (~42–57% r.h.). The straight lines represent linear regressions of the data with their 95% confidence limits (dashed lines).

Surface concentrations of adsorbed nitric acid, $[HNO_3]_{surface}$ (molecules cm^{-2}), measured after the experiments, were assumed to be constant during each experiment, since the HNO_3 source was running continuously. Thus, $J(HNO_3 \rightarrow HONO)$ was calculated from the slope of a plot of the measured average surface flux density ($\Delta[HONO]_{surface}/\Delta t$) against $[HNO_3]_{surface}$:

$$\frac{\Delta[HONO]_{surface}}{\Delta t} = J(HNO_3 \rightarrow HONO) \times [HNO_3]_{surface}. \quad (2)$$

From weighted orthogonal regression plots according to eqn (2) and after correction for gas-phase photolysis of HONO, photolysis frequencies $J(HNO_3 \rightarrow HONO)$ of $(1.24 \pm 0.19) \times 10^{-6}$ s^{-1} and $(3.4 \pm 1.8) \times 10^{-7}$ s^{-1} were determined at ~50% r.h. for the short- (sw) and the long-wavelength (lw) setups, respectively, (see Fig. 5). In between the experimental errors photolysis frequencies were found to be independent of the gas flow rate. The measured values are much lower than those obtained in another study on HONO formation from the photolysis of adsorbed HNO_3 on glass surfaces,[24] for which photolysis frequencies of $\sim 10^{-5}$ s^{-1} were calculated under atmospheric conditions. The difference between the two studies is actually even higher, since the small values determined in the present study are still upper limits as the lamps used in the experiments have higher actinic fluxes compared to the atmosphere (see Fig. 2, Table 1 and Section 4). Potential underestimation of the surface area of the used quartz tube, *e.g.* by any surface roughness, will not affect the measured $J(HNO_3 \rightarrow HONO)$ since the surface area cancels out in eqn (2) in the two terms $\Delta[HONO]_{surface}$ and $[HNO_3]_{surface}$. In addition, the potential inhomogeneous surface concentration throughout the flow tube would also not affect the measured $J(HNO_3)$, since first order kinetics was observed.

3.3. Wavelength dependency

To estimate the atmospheric implication of the HNO_3 photolysis, the results obtained in laboratory experiments cannot be used directly, since the actinic flux spectra of laboratory systems are typically very different from those of the atmosphere (*cf.* Fig. 2). To calculate atmospherically relevant HNO_3 photolysis frequencies for HONO formation according to:

$$J(HNO_3 \rightarrow HONO) = \sum_{\lambda_1}^{\lambda_n} F_\lambda \times \sigma(HNO_3)_\lambda \times \phi(HNO_3 \rightarrow HONO)_\lambda \times \Delta\lambda, \quad (3)$$

spectroscopic information on the absorption cross-section ($\sigma(HNO_3)_\lambda$), the quantum yield ($\phi(HNO_3 \rightarrow HONO)_\lambda$) and the actinic flux spectra (F_λ) of the laboratory system and the atmosphere are necessary. Since the absorption cross-sections and quantum yields are still uncertain, extrapolation to atmospheric conditions, as done in another study,[24] is highly questionable. To better estimate the atmospheric implications of HNO_3 photolysis, a limited wavelength dependence of the HONO formation was investigated in the present study using two different sets of lamps (see Fig. 5), for which the spectra are shifted by ~20 nm (see Fig. 2). The ratio of the experimentally determined photolysis frequency, $J(HNO_3 \rightarrow HONO)_{sw}/J(HNO_3 \rightarrow HONO)_{lw}$, of 3.6 (see Section 3.2) is much lower compared to theoretical ratios of 10.9 and 14.1 for the liquid- and gas-phase photolysis, respectively. The latter was calculated using eqn (3) and known liquid-[60] and gas-phase[51] absorption cross-sections, measured actinic fluxes and assuming a wavelength independent quantum yield.[49] This result is another indication of surface photolysis of HNO_3 and thus confirms recent publications on a red-shift of the $n \rightarrow \pi^*$ absorption of adsorbed HNO_3.[45,47] Using these published cross-sections, measured HONO formation (see Fig. 5) and actinic fluxes (see Fig. 2), formal quantum yields for HONO formation, $\phi(HNO_3 \rightarrow HONO)$, for the heterogeneous photolysis reaction (R1) of 6.9×10^{-5} and 8.4×10^{-5} were calculated using eqn (3) for the short- and long-wavelength setups, respectively. Taking into account the uncertainties of the measured HONO formation, actinic flux spectra and published absorption cross-sections, the similarity of the two values indicates no strong wavelength dependence of the quantum yield, and thus an average value of $\phi(HNO_3 \rightarrow HONO) = (7.6 \pm 1.5) \times 10^{-5}$ is preferred and applied in further calculations.

3.4. Influence of relative humidity

Similar to the study by Zhou *et al.*,[24] a strong influence of the relative humidity on the HONO formation inside the flow-reactor was observed. HONO immediately decreased to very low levels after stopping the humidifier, indicating a direct influence of water on the HONO production. There are different potential explanations for this observation: (i) photochemical HONO formation is active only for H_2O/HNO_3 clusters[26] and/or (ii) is caused by secondary chemistry *via* the additional reaction product NO_2, for which strong humidity dependence of the heterogeneous HONO formation is known.[61]

3.5. NO_2 dependency

To distinguish between these two explanations, the NO_2 dependence of the HONO formation was studied. Besides HONO, NO_2 is a main product of the HNO_3 photolysis (see Fig. 3):

$$HNO_3(ads.) + h\nu \xrightarrow{J(HNO_3 \rightarrow NO_2)} NO_2 + OH. \quad (R2)$$

Open Access Article. Published on 09 marzo 2016. Downloaded on 30/09/2025 1:16:36 a.m..
This article is licensed under a Creative Commons Attribution 3.0 Unported Licence.

Thus, in addition to possible direct HONO formation *via* HNO_3 photolysis (R1), the reaction product NO_2 may also form HONO *via* secondary heterogeneous conversion:[61]

$$2NO_2 + H_2O \xrightarrow{\text{surface}} HONO + HNO_3, \qquad (R3)$$

or by the reaction of NO_2 with chemisorbed water on the reactor surfaces:[62]

$$2NO_2 + H_{chem} + OH_{chem} \xrightarrow{\text{surface}} HONO + HNO_3. \qquad (R4)$$

Furthermore, formation of electronically excited NO_2 was recently proposed in the photolysis of adsorbed HNO_3 on aluminium surfaces, which may react with adsorbed water:[46,48]

$$NO_2^* + H_2O \xrightarrow{\text{surface}} HONO + OH. \qquad (R5)$$

Finally, based on theoretical calculations, photolysis of complexes of HNO_3 with nitrogen oxides has been proposed to explain HONO formation by the photolysis of adsorbed HNO_3.[63]

To elucidate the contribution of NO_2 to the observed HONO formation, NO_2 was added to the reaction mixtures (see Fig. 3). From this and other similar experiments total HONO production rates were calculated from the concentration differences between the flow-reactor bypass and the dark or light steps, respectively, and plotted against the final NO_x level at the flow-reactor exit (see Fig. 6). NO_x was used here instead of the proposed precursor NO_2 to take into account the significant NO_2 photolysis in the flow-reactor (see Table 1). Thus, NO measured at the exit of the reactor mainly originated from the fast gas-phase photolysis of NO_2:

$$NO_2 + h\nu \rightarrow NO + O(^3P), \qquad (R6)$$

and was available as a reactant for heterogeneous HONO formation, reactions (R3)–(R5).

Two important conclusions can be drawn from the experimental data:

(a) HONO formation depends strongly on the NO_2 concentration and within the error of the intercept ($\pm 2 \times 10^8$ molecules cm^{-2} s^{-1}) extrapolation to 0 ppbV NO_x indicates no additional HONO formation by HNO_3 photolysis alone (R1) under the experimental conditions applied. Thus, it is proposed that the observed HONO formation is caused by the heterogeneous conversion of NO_2 on the reactor surfaces, reactions (R3) or (R4).

(b) HONO formation by heterogeneous NO_2 conversion in the dark and under irradiation is similar, confirming a proposed dark formation of HONO, *e.g.* by reaction (R3) on clean quartz glass surfaces. This result is in excellent agreement with other studies,[26,44] in which no photoenhancement of reaction (R3) was observed. Thus, the experimental results of the present study do not confirm photochemical HONO formation *via* excited NO_2, reaction (R5), as proposed in another study by Abida *et al.*[48] when using excimer laser photolysis. Very recently, the same group[64] also excluded the direct formation of excited NO_2 at least for the gas-phase photolysis of HNO_3 and proposed secondary HONO formation by the heterogeneous reaction (R3). This conclusion is in agreement with studies of reaction (R5) in the gas phase,[35,36] in which HONO formation *via* excited NO_2 was excluded at atmospherically relevant actinic fluxes. Finally, the missing light-enhancement also excludes photolysis of complexes of HNO_3 with nitrogen oxides as sources of HONO.[63]

Based on these two conclusions a two-step formation mechanism of HONO is proposed here. First, NO_2 is formed in the photolysis of adsorbed HNO_3, reaction (R2), at longer wavelengths compared to the gas and liquid phases. Second, NO_2 is consecutively converted into HONO *via* the heterogeneous dark reactions (R3) or (R4) on the pure quartz glass surfaces. This consecutive formation of HONO *via* the intermediate NO_2 was already proposed for the photolysis of nitrate in snow[22,65] and in the aqueous phase.[66] However, for snow the significant red-shift of the nitrate absorption compared to the liquid nitrate spectra was not observed leading to negligible NO_x formation at wavelengths >345 nm.[67] Finally, the observed NO formation (see Fig. 3) is explained by the gas-phase photolysis of NO_2, reaction (R6).

To determine HNO_3 photolysis frequencies for the primary reaction product NO_2:

$$J(HNO_3 \rightarrow NO_2) = \sum_{\lambda_1}^{\lambda_n} F_\lambda \times \sigma(HNO_3)_\lambda \times \phi(HNO_3 \rightarrow NO_2)_\lambda \times \Delta\lambda, \qquad (4)$$

the sum of photochemically formed NO_2, HONO and NO was considered in calculations similar to eqn (2). Using weighted orthogonal linear regression plots, photolysis frequencies $J(HNO_3 \rightarrow NO_2)$ of $(6.6 \pm 1.3) \times 10^{-6}$ s^{-1} and $(1.3 \pm 1.0) \times 10^{-6}$ s^{-1} were determined at $\sim$50% r.h. for the short and the long wavelength setups, respectively.

Using the absorption cross-sections of adsorbed HNO_3 from the studies of Zhu *et al.*[45] and Du and Zhu,[47] measured actinic fluxes of both setups and measured values of $J(HNO_3 \rightarrow NO_2)$ from the present study, similar quantum yields for NO_2 formation, $\phi(HNO_3 \rightarrow NO_2)$, of $(3.6 \pm 0.8) \times 10^{-4}$ and $(3.2 \pm 2.5) \times 10^{-4}$ were determined for the short and the long wavelength setups, respectively. The averaged quantum yield for both

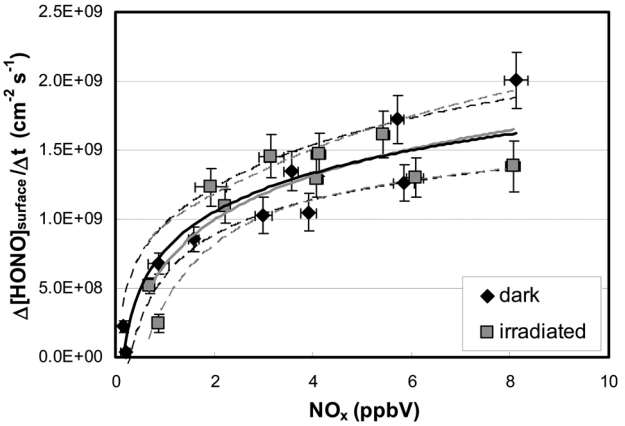

Fig. 6 HONO flux as a function of the NO_x concentration calculated from the differences (dark-bypass) and (illuminated-bypass), ($[HNO_3]_{surf} \leq 0.8 \times 10^{14}$ cm^{-2}, 51–54% r.h.). Within the experimental errors (95% confidence intervals, dashed lines), logarithmic fits (solid lines) show no difference between HONO formation in the dark (black) and under illumination (grey).

This journal is © the Owner Societies 2016

Open Access Article. Published on 09 marzo 2016. Downloaded on 30/09/2025 1:16:36 a.m..
This article is licensed under a Creative Commons Attribution 3.0 Unported Licence.

setups of $(3.4 \pm 2.6) \times 10^{-4}$ is orders of magnitude lower compared to the studies of Zhu *et al.*[46] and Abida *et al.*,[48] in which quantum yields near unity were observed in excimer laser photolysis experiments at 308 and 351 nm. Reasons for the strong discrepancy are still unclear and may be explained by:

(a) Overestimation of the HNO_3 absorption cross-sections in the studies of Zhu *et al.*[45] and Du and Zhu.[47] In these studies, the concentrations of adsorbed HNO_3 were only indirectly determined by adsorption isotherms based on measured light absorption and by using an estimated van der Waals radius for HNO_3 resulting in a monolayer coverage only at very high gas-phase levels (15–20 ppmV) of the highly sticky HNO_3. In contrast, in the present study three orders of magnitude lower gas-phase concentrations ($\sim$10 ppbV) were necessary to obtain similar levels of adsorbed HNO_3, which were directly measured by ion chromatography. If surface levels of HNO_3 were much higher than proposed in the studies of Zhu *et al.*[45] and Du and Zhu,[47] absorption cross-sections may be overestimated, which was also recently proposed by Tadić;[68]

(b) Overestimation of the quantum yields $\phi(HNO_3 \rightarrow NO_2)$ in the studies of Zhu *et al.*[46] and Abida *et al.*[48] caused by higher photon flux densities of the excimer laser used for the photolysis experiments compared to atmospheric conditions. High photon flux densities may have caused stronger NO_2 formation, *e.g.* by a potential multi-photon excitation, which was also recently observed for the gas-phase reaction of $NO_2^* + H_2O$.[36]

Independent of which explanation is correct, photolysis of pure HNO_3 will be of much lower importance for renoxification than previously assumed, since the presented NO_2 flux densities were determined under realistic atmospheric conditions (HNO_3 level, humidity, actinic flux). A strong indication for an overestimation of either the absorption cross-sections or the quantum yield of adsorbed HNO_3 in the former studies[45–47] is the resulting unrealistic short photolytic lifetime of adsorbed HNO_3 of only $\sim$5 min (see Section 4). If published absorption cross-sections are overestimated, our calculated quantum yields, which are based on these values, will be strongly underestimated.

3.6. Influence of VOCs

To explain enhanced HONO formation, photosensitized conversion of HNO_3/nitrate by adsorbed organic compounds was recently proposed.[69–72] In addition, increased HONO formation by scavenging of OH radicals formed *via* reaction (R2) by organic compounds was proposed for the liquid phase photolysis of nitrate.[66] To test the influence of organic compounds on the reaction system, in one experiment a GC calibration mixture of 29 VOCs ($\leq$C10, see Section 2.3. for details; each with a final mixing ratio of 3–4 ppbV) was continuously added to the humidified HNO_3 mixture, both, during surface saturation overnight and during the photolysis. While some of the used VOCs clearly do not adsorb onto surfaces (*e.g.* C1–C4), others are expected to be surface active (*e.g.* β-pinene, limonene, xylenes, *n*-butanol, methacrolein) and substituted aromatic compounds are even proposed to participate in redox reactions of NO_y.[18] However, within the experimental errors photochemical HONO formation was not enhanced compared to the absence of the VOCs. A similar result was obtained when the flow tube was not cleaned after flushing with laboratory air for one day before the photolysis experiment. Thus, at least for the smaller VOCs and at atmospherically relevant concentrations, HONO formation by photosensitized conversion of HNO_3 could not be confirmed. However, further experiments using more complex VOCs, known as photosensitizers (*e.g.* aromatic carbonyls, hydroxy-PAHs, humic acid *etc.*), are recommended in the future.

4. Atmospheric implications

Based on the experimental results HONO formation from the photolysis of adsorbed nitric acid was estimated under typical atmospheric conditions. The present study indicates no direct photochemical HONO formation *via* reaction (R1), but secondary formation by the heterogeneous dark conversion of NO_2 on humid surfaces, reaction (R3) or (R4). At high NO_x levels, reaction (R3) can be a significant night-time ground surface source of HONO in the atmosphere,[12,61] but is too slow to explain daytime HONO levels.[41] Here, other NO_2 reactions, *e.g.* the photosensitized conversion on humic acid surfaces have been proposed.[19,20]

Although HONO is not the primary HNO_3 photolysis product, reaction (R1), the formal quantum yield for HONO formation of $\phi(HNO_3 \rightarrow HONO) = (7.6 \pm 1.5) \times 10^{-5}$, as determined in Section 3.3., was considered here. Using this wavelength independent quantum yield, published absorption cross-sections of adsorbed HNO_3[45,47] and the upper limit actinic flux in the atmosphere at 0° SZA[50] a formal photolysis frequency $J(HNO_3 \rightarrow HONO)$ of only 2.4×10^{-7} s^{-1} was derived using eqn (3). This value is almost two orders of magnitude lower compared to another laboratory study by Zhou and coworkers,[24] in which atmospheric HONO formation in a rural environment could be well explained by reaction (R1). In contrast, using the results of the present study and assuming a high surface coverage of HNO_3 on atmospheric surfaces of 10^{14} cm^{-2} ($\sim$one monolayer[45]), an upper limit HONO flux density of only 2.4×10^7 cm^{-2} s^{-1} can be calculated using eqn (1) at 0° SZA. This upper limit is 2–3 orders of magnitude lower compared to HONO flux densities typically observed over irradiated surfaces in the atmosphere.[25,42,43] Thus, HONO formation by photolysis of pure HNO_3 is too slow to explain field observations, even in rural environments. Reasons for the strong discrepancy between the present study and the one by Zhou *et al.*[24] are yet unclear but may possibly be explained by:

(a) the indirect extrapolation of the laboratory results to the atmosphere *via* the chemical actinometry used by Zhou *et al.*,[24] by which OH radicals formed in the liquid phase photolysis of nitrate were used to quantify $J(HNO_3)$ for the red-shifted (compared to the liquid phase) photolysis of adsorbed HNO_3.[45,47] In contrast, in the present study a well calibrated spectroradiometer was used to quantify actinic fluxes and to calculate $J(HNO_3)$ using eqn (3). Here, the wavelength dependent absorption cross-sections of adsorbed HNO_3[45,47] were considered;

(b) different surface properties of the reactors and the different NO_2 levels used. While in the present experiments, the flow-reactor was chemically cleaned by HF prior to each experiment,

Open Access Article. Published on 09 marzo 2016. Downloaded on 30/09/2025 1:16:36 a.m..
This article is licensed under a Creative Commons Attribution 3.0 Unported Licence.

impurities on irradiated surfaces and higher NO_2 levels in the experiments by Zhou *et al.*[24] may have caused increased HONO yields *via* reaction (R3) and (R4), or by photosensitized conversion of NO_2 on adsorbed organic impurities.[18–21] Alternatively, direct photosensitized conversion of HNO_3/nitrate by organic impurities[69–72] may also be another explanation for the higher HONO yields observed by Zhou *et al.*[24]

However, in the present study the latter mechanism could not be confirmed at least for a mixture of 29 smaller VOCs ($\leq$C10) or when the reactor was not cleaned after flushing with laboratory air for one day before the experiment. Thus, in the future, HONO formation from the photolysis of adsorbed HNO_3 should be studied on more realistic organic surfaces, for example, on leaves, urban grime or humic acid. However, for the photolysis of pure HNO_3 adsorbed on non-reactive surfaces, HONO formation is of minor importance.

Similar conclusions can be drawn for a possible renoxification by photolysis of pure adsorbed HNO_3 in the absence of photosensitizers. Extrapolation of the experimental results from the present study to atmospheric conditions (see above) yields an upper photolysis frequency limit of $J(HNO_3 \rightarrow NO_2) = 1.1 \times 10^{-6}\ s^{-1}$ (0° SZA). This value translates into photolytic lifetimes of HNO_3 on surfaces of $\sim$30 days when the diurnal variability of the actinic flux in the atmosphere is considered. This contrasts starkly with an atmospheric photolytic lifetime of adsorbed HNO_3 of only $\sim$5 min (0° SZA), which is derived when published cross-sections and quantum yields are used.[48] Such a short lifetime is highly unreasonable and would result in negligible amounts of nitrates on atmospheric surfaces during daytime, which is not in agreement with direct field observations.[25]

Summary

In the present study heterogeneous formation of nitrous acid (HONO) from photolysis of adsorbed HNO_3 was studied in a photo flow-reactor, from which a HNO_3 photolysis frequency for HONO formation, $J(HNO_3 \rightarrow HONO)$, of only $2.4 \times 10^{-7}\ s^{-1}$ is extrapolated for atmospheric noontime conditions (0° SZA). The slow HONO formation is explained by secondary heterogeneous formation *via* the primary HNO_3 photolysis product NO_2. On pure quartz glass surfaces, the heterogeneous conversion of NO_2 into HONO shows no photoenhancement, in good agreement with other studies in simulation chambers.

For the primary photolysis product NO_2 a low photolysis frequency of $J(HNO_3 \rightarrow NO_2) = 1.1 \times 10^{-6}\ s^{-1}$ (0° SZA) is calculated. From the wavelength dependence of the HONO formation a red-shift of the UV absorption of adsorbed HNO_3 is inferred in agreement with other recent studies. However, in contrast to these studies, it is concluded that photolysis of pure adsorbed HNO_3 is only a minor source of HONO and NO_2 in the atmosphere, at least on non-reactive substrates. For the future, HONO formation by the photolysis of adsorbed HNO_3 should also be studied on more complex surfaces, for example, on leaves, urban grime or humic acid.

Acknowledgements

The financial support for this work by the Deutsche Forschungsgemeinschaft (DFG) under contract number (KL 1392/3-1) is gratefully acknowledged.

References

1 X. Zhou, K. Civerolo, H. Dai, G. Huang, J. Schwab and K. L. Demerjian, Summertime Nitrous Acid Chemistry in the Atmospheric Boundary Layer at a Rural Site in New York State, *J. Geophys. Res.*, 2002, **107**, 4590.
2 K. Acker, D. Möller, W. Wieprecht, F. X. Meixner, B. Bohn, S. Gilge, C. Plass-Dülmer and H. Berresheim, Strong Daytime Production of OH from HNO_2 at a Rural Mountain Site, *Geophys. Res. Lett.*, 2006, **33**, L02809.
3 M. Sörgel, I. Trebs, A. Serafimovich, A. Moravek, A. Held and C. Zetzsch, Simultaneous HONO Measurements in and above a Forest Canopy: Influence of Turbulent Exchange on Mixing Ratio Differences, *Atmos. Chem. Phys.*, 2011, **11**, 841–855.
4 G. Villena, P. Wiesen, C. A. Cantrell, F. Flocke, A. Fried, S. R. Hall, R. S. Hornbrook, D. Knapp, E. Kosciuch, R. L. Mauldin III, J. A. McGrath, D. Montzka, D. Richter, K. Ullmann, J. Walega, P. Weibring, A. Weinheimer, R. M. Staebler, J. Liao, L. G. Huey and J. Kleffmann, Nitrous Acid (HONO) during Polar Spring in Barrow, Alaska: A net Source of OH Radicals?, *J. Geophys. Res.: Atmos.*, 2011, **116**, D00R07.
5 R. Oswald, M. Ermel, K. Hens, A. Novelli, H. G. Ouwersloot, P. Paasonen, T. Petäjä, M. Sipilä, P. Keronen, J. Bäck, R. Königstedt, Z. Hosaynali Beygi, H. Fischer, B. Bohn, D. Kubistin, H. Harder, M. Martinez, J. Williams, T. Hoffmann, I. Trebs and M. Sörgel, Comparison of HONO Budgets for two Measurement Heights at a Field Station within the Boreal Forest in Finland, *Atmos. Chem. Phys.*, 2015, **15**, 799–813.
6 A. Neftel, A. Blatter, R. Hesterberg and T. Staffelbach, Measurements of Concentration Gradients of HNO_2 and HNO_3 over a Semi-Natural Ecosystem, *Atmos. Environ.*, 1996, **30**, 3017–3025.
7 T. Staffelbach, A. Neftel, A. Blatter, A. Gut, M. Fahrni, J. Stähelin, A. Prévôt, A. Hering, M. Lehning, B. Neininger, M. Bäumle, G. L. Kok, J. Dommen, M. Hutterli and M. Anklin, Photochemical Oxidant Formation Over Southern Switzerland 1. Results from Summer 1994, *J. Geophys. Res.*, 1997, **102**, 23345–23362.
8 J. Kleffmann, T. Gavriloaiei, A. Hofzumahaus, F. Holland, R. Koppmann, L. Rupp, E. Schlosser, M. Siese and A. Wahner, Daytime Formation of Nitrous Acid: A Major Source of OH-Radicals in a Forest, *Geophys. Res. Lett.*, 2005, **32**, L05818.
9 V. Michoud, A. Colomb, A. Borbon, K. Miet, M. Beekmann, M. Camredon, B. Aumont, S. Perrier, P. Zapf, G. Siour, W. Ait-Helal, C. Afif, A. Kukui, M. Furger, J. C. Dupont, M. Haeffelin and J. F. Doussin, Study of the Unknown

Open Access Article. Published on 09 marzo 2016. Downloaded on 30/09/2025 1:16:36 a.m..
This article is licensed under a Creative Commons Attribution 3.0 Unported Licence.

HONO Daytime Source at a European Suburban Site during the MEGAPOLI Summer and Winter Field Campaigns, *Atmos. Chem. Phys.*, 2014, **14**, 2805–2822.

10 J. Kleffmann, J. Heland, R. Kurtenbach, J. C. Lörzer and P. Wiesen, A new Instrument (LOPAP) for the Detection of Nitrous acid (HONO), *Environ. Sci. Pollut. Res.*, 2002, **9**(special issue 4), 48–54.

11 X. Ren, H. Harder, M. Martinez, R. L. Lesher, A. Oliger, J. B. Simpas, W. H. Brune, J. J. Schwab, K. L. Demerjian, Y. He, X. Zhou and H. Gao, OH and HO_2 Chemistry in the Urban Atmosphere of New York City, *Atmos. Environ.*, 2003, **37**, 3639–3651.

12 B. Vogel, H. Vogel, J. Kleffmann and R. Kurtenbach, Measured and Simulated Vertical Profiles of Nitrous Acid – Part II, Model Simulations and Indications for a Photolytic Source, *Atmos. Environ.*, 2003, **37**, 2957–2966.

13 K. Acker, A. Febo, S. Trick, C. Perrino, P. Bruno, P. Wiesen, D. Möller, W. Wieprecht, R. Auel, M. Guisto, A. Geyer, U. Platt and I. Allegrini, Nitrous Acid in the Urban Area of Rome, *Atmos. Environ.*, 2006, **40**, 3123–3133.

14 X. Ren, W. H. Brune, J. Mao, M. J. Mitchell, R. L. Lesher, J. B. Simpas, A. R. Metcalf, J. J. Schwab, C. Cai, Y. Li, K. L. Demerjian, H. D. Felton, G. Boynton, A. Adams, J. Perry, Y. He, X. Zhou and J. Hou, Behavior of OH and HO_2 in the Winter Atmosphere in New York City, *Atmos. Environ.*, 2006, **40**(supplement 2), 252–263.

15 Y. F. Elshorbany, R. Kurtenbach, P. Wiesen, E. Lissi, M. Rubio, G. Villena, E. Gramsch, A. R. Rickard, M. J. Pilling and J. Kleffmann, Oxidation Capacity of the City Air of Santiago, Chile, *Atmos. Chem. Phys.*, 2009, **9**, 2257–2273.

16 Y. F. Elshorbany, J. Kleffmann, R. Kurtenbach, E. Lissi, M. Rubio, G. Villena, E. Gramsch, A. R. Rickard, M. J. Pilling and P. Wiesen, Seasonal Dependence of the Oxidation Capacity of the City of Santiago de Chile, *Atmos. Environ.*, 2010, **44**, 5383–5394.

17 F. Hendrick, J.-F. Müller, K. Clémer, P. Wang, M. De Mazière, C. Fayt, C. Gielen, C. Hermans, J. Z. Ma, G. Pinardi, T. Stavrakou, T. Vlemmix and M. Van Roozendael, Four Years of Ground-based MAX-DOAS Observations of HONO and NO_2 in the Beijing Area, *Atmos. Chem. Phys.*, 2014, **14**, 765–781.

18 C. George, R. S. Strekowski, J. Kleffmann, K. Stemmler and M. Ammann, Photoenhanced Uptake of Gaseous NO_2 on Solid Organic Compounds: A Photochemical Source of HONO?, *Faraday Discuss.*, 2005, **130**, 195–210.

19 K. Stemmler, M. Ammann, C. Dondors, J. Kleffmann and C. George, Photosensitized Reduction of Nitrogen Dioxide on Humic Acid as a Source of Nitrous Acid, *Nature*, 2006, **440**, 195–198.

20 K. Stemmler, M. Ndour, Y. Elshorbany, J. Kleffmann, B. D'Anna, C. George, B. Bohn and M. Ammann, Light Induced Conversion of Nitrogen Dioxide into Nitrous Acid on Submicron Humic Acid Aerosol, *Atmos. Chem. Phys.*, 2007, **7**, 4237–4248.

21 Y. Sosedova, A. Rouvière, T. Bartels-Rausch and M. Ammann, UVA/Vis-induced Nitrous Acid Formation on Polyphenolic Films Exposed to Gaseous NO_2, *Photochem. Photobiol. Sci.*, 2011, **10**, 1680–1690.

22 X. Zhou, H. J. Beine, R. E. Honrath, J. D. Fuentes, W. Simpson, P. B. Shepson and J. W. Bottenheim, Snowpack Photochemical Production of HONO: A major Source of OH in the Arctic Boundary Layer in Springtime, *Geophys. Res. Lett.*, 2001, **28**, 4087–4090.

23 X. Zhou, Y. He, G. Huang, T. D. Thornberry, M. A. Carroll and S. B. Bertman, Photochemical Production of Nitrous Acid on Glass Sample Manifold Surface, *Geophys. Res. Lett.*, 2002, **29**(14), 1681.

24 X. Zhou, H. Gao, Y. He, G. Huang, S. B. Bertman, K. Civerolo and J. Schwab, Nitric Acid Photolysis on Surfaces in Low-NO_x Environments: Significant Atmospheric Implications, *Geophys. Res. Lett.*, 2003, **30**, 2217.

25 X. Zhou, N. Zhang, M. TerAvest, D. Tang, J. Hou, S. Bertman, M. Alaghmand, P. B. Shepson, M. A. Caroll, S. Griffith, S. Dusanter and P. S. Stevens, Nitric Acid Photolysis on Forest Canopy Surface as a Source for Tropospheric Nitrous Acid, *Nat. Geosci.*, 2011, **4**, 440–443.

26 K. A. Ramazan, D. Syomin and B. J. Finlayson-Pitts, The Photochemical Production of HONO during the Heterogeneous Hydrolysis of NO_2, *Phys. Chem. Chem. Phys.*, 2004, **6**, 3836–3843.

27 H. Su, Y. Cheng, R. Oswald, T. Behrendt, I. Trebs, F. X. Meixner, M. O. Andreae, P. Cheng, Y. Zhang and U. Pöschl, Soil Nitrite as a Source of Atmospheric HONO and OH Radicals, *Science*, 2011, **333**, 1616–1618.

28 R. Oswald, T. Behrendt, M. Ermel, D. Wu, H. Su, Y. Cheng, C. Breuninger, A. Moravek, E. Mougin, C. Delon, B. Loubet, A. Pommerening-Röser, M. Sörgel, U. Pöschl, T. Hoffmann, M. O. Andreae, F. X. Meixner and I. Trebs, HONO Emissions from Soil Bacteria as a Major Source of Atmospheric Reactive Nitrogen, *Science*, 2013, **341**, 1233–1235.

29 M. Maljanen, P. Yli-Pirilä, J. Hytönen and J. Joutsensaari, Acidic Northern Soils as a Source of Atmospheric Nitrous Acid (HONO), *Soil Biol. Biochem.*, 2013, **67**, 94–97.

30 D. Wu, C. J. Kampf, U. Pöschl, U. Oswald, J. Cui, M. Ermel, C. Hu, I. Trebs and M. Sörgel, Novel Tracer Method to Measure Isotopic Labeled Gas-phase Nitrous Acid ($HO^{15}NO$) in Biogeochemical Studies, *Environ. Sci. Technol.*, 2014, **48**, 8021–8027.

31 M. A. Donaldson, A. E. Berke and J. D. Raff, Uptake of Gas Phase Nitrous Acid onto Boundary Layer Soil Surfaces, *Environ. Sci. Technol.*, 2013, **48**, 375–383.

32 T. C. VandenBoer, S. S. Brown, J. G. Murphy, W. C. Keene, C. J. Young, A. A. P. Pszenny, S. Kim, C. Warneke, J. A. de Gouw, J. R. Maben, N. L. Wagner, T. P. Riedel, J. A. Thornton, D. E. Wolfe, W. P. Dubé, F. Öztürk, C. A. Brock, N. Grossberg, B. Lefer, B. Lerner, A. M. Middlebrook and J. M. Roberts, Understanding the Role of the Ground Surface in HONO Vertical Structure: High Resolution Vertical Profiles during NACHTT-11, *J. Geophys. Res.: Atmos.*, 2013, **118**, 10155–10171.

33 T. C. VandenBoer, M. Z. Markovic, J. E. Sanders, X. Ren, S. E. Pusede, E. C. Browne, R. C. Cohen, L. Zhang,

Open Access Article. Published on 09 marzo 2016. Downloaded on 30/09/2025 1:16:36 a.m..
This article is licensed under a Creative Commons Attribution 3.0 Unported Licence.

J. Thomas, W. H. Brune and J. G. Murphy, Evidence for a Nitrous Acid (HONO) Reservoir at the Ground Surface in Bakersfield, CA, during CALNex 2010, *J. Geophys. Res.: Atmos.*, 2014, **119**, 9093–9106.

34 S. Li, J. Matthews and A. Sinha, Atmospheric Hydroxyl Radical Production from Electronically Excited NO_2 and H_2O, *Science*, 2008, **319**, 1657–1660.

35 J. N. Crowley and S. A. Carl, OH Formation in the Photoexcitation of NO_2 Beyond the Dissociation Threshold in the Presence of Water Vapor, *J. Phys. Chem. A*, 1997, **101**, 4178–4184.

36 D. Amedro, A. E. Parker, C. Schoemaecker and C. Fittschen, Direct Observation of OH Radicals after 565 nm Multiphoton Excitation of NO_2 in the Presence of H_2O, *Chem. Phys. Lett.*, 2011, **513**, 12–16.

37 I. Bejan, Y. Abd El Aal, I. Barnes, T. Benter, B. Bohn, P. Wiesen and J. Kleffmann, The Photolysis of Ortho-Nitrophenols: A New Gas Phase Source of HONO, *Phys. Chem. Chem. Phys.*, 2006, **8**, 2028–2035.

38 X. Li, F. Rohrer, A. Hofzumahaus, T. Brauers, R. Häseler, B. Bohn, S. Broch, H. Fuchs, S. Gomm, F. Holland, J. Jäger, J. Kaiser, F. N. Keutsch, I. Lohse, K. Lu, R. Tillmann, R. Wegener, G. M. Wolfe, T. F. Mentel, A. Kiendler-Scharr and A. Wahner, Missing Gas-phase Source of HONO Inferred from Zeppelin Measurements in the Troposphere, *Science*, 2014, **344**, 292–296.

39 X. Li, F. Rohrer, A. Hofzumahaus, T. Brauers, R. Häseler, B. Bohn, S. Broch, H. Fuchs, S. Gomm, F. Holland, J. Jäger, J. Kaiser, F. N. Keutsch, I. Lohse, K. Lu, R. Tillmann, R. Wegener, G. M. Wolfe, T. F. Mentel, A. Kiendler-Scharr and A. Wahner, Response to Comment on ''Missing Gas-Phase Source of HONO Inferred from Zeppelin Measurements in the Troposphere'', *Science*, 2015, **348**, 1326e.

40 C. Ye, X. Zhou, D. Pu, J. Stutz, J. Festa, M. Spolaor, C. Cantrell, R. L. Mauldin, A. Weinheimer and J. Haggerty, Comment on ''Missing Gas-phase Source of HONO Inferred from Zeppelin Measurements in the Troposphere'', *Science*, 2015, **348**, 1326d.

41 J. Kleffmann, Daytime Sources of Nitrous Acid (HONO) in the Atmospheric Boundary Layer, *ChemPhysChem*, 2007, **8**, 1137–1144.

42 X. Ren, J. E. Sanders, A. Rajendran, R. J. Weber, A. H. Goldstein, S. E. Pusede, E. C. Browne, K.-E. Min and R. C. Cohen, A Relaxed Eddy Accumulation System for Measuring Vertical Fluxes of Nitrous Acid, *Atmos. Meas. Tech.*, 2011, **4**, 2093–2103.

43 N. Zhang, X. Zhou, S. Bertman, D. Tang, M. Alaghmand, P. B. Shepson and M. A. Carroll, Measurements of Ambient HONO Concentrations and Vertical HONO Flux above a Northern Michigan Forest Canopy, *Atmos. Chem. Phys.*, 2012, **12**, 8285–8296.

44 F. Rohrer, B. Bohn, T. Brauers, D. Brüning, F.-J. Johnen, A. Wahner and J. Kleffmann, Characterisation of the Photolytic HONO-source in the Atmosphere Simulation Chamber SAPHIR, *Atmos. Chem. Phys.*, 2005, **5**, 2189–2201.

45 C. Zhu, B. Xiang, L. Zhu and R. Cole, Determination of Absorption Cross Sections of Surface-adsorbed HNO_3 in the 290–330 nm Region by Brewster Angle Cavity Ring-down Spectroscopy, *Chem. Phys. Lett.*, 2008, **458**, 373–377.

46 C. Zhu, B. Xiang, L. T. Chu and L. Zhu, 308 nm Photolysis of Nitric Acid in the Gas Phase, on Aluminum Surfaces, and on Ice Films, *J. Phys. Chem. A*, 2010, **114**, 2561–2568.

47 J. Du and L. Zhu, Quantification of the Absorption Cross Sections of Surface-adsorbed Nitric Acid in the 335–365 nm Region by Brewster Angle Cavity Ring-down Spectroscopy, *Chem. Phys. Lett.*, 2011, **511**, 213–218.

48 O. Abida, J. Du and L. Zhu, Investigation of the Photolysis of the Surface-adsorbed HNO_3 by Combining Laser Photolysis with Brewster Angle Cavity Ring-down Spectroscopy, *Chem. Phys. Lett.*, 2012, **534**, 77–82.

49 E. P. Gardner, G. D. Sperry and J. G. Calvert, Primary Quantum Yields of NO_2 Photodissociation, *J. Geophys. Res.*, 1987, **92**, 6642–6652.

50 B. J. Finlayson-Pitts and J. N. Pitts Jr., *Chemistry of the Upper and Lower Atmosphere: Theory, Experiments, and Applications*, Academic Press, 2000.

51 R. Atkinson, D. L. Baulch, R. A. Cox, J. N. Crowley, R. F. Hampson, R. G. Hynes, M. E. Jenkin, M. J. Rossi and J. Troe, Evaluated Kinetic and Photochemical Data for Atmospheric Chemistry: Volume I – Gas Phase Reactions of O_x, HO_x, NO_x and SO_x Species, *Atmos. Chem. Phys.*, 2004, **4**, 1461–1738.

52 R. Atkinson, D. L. Baulch, R. A. Cox, J. N. Crowley, R. F. Hampson, R. G. Hynes, M. E. Jenkin, M. J. Rossi and J. Troe, Evaluated Kinetic and Photochemical Data for Atmospheric Chemistry: Volume II – Gas Phase Reactions of Organic Species, *Atmos. Chem. Phys.*, 2006, **6**, 3625–4055.

53 J. Stutz, E. S. Kim, U. Platt, P. Bruno, C. Perrino and A. Febo, UV-visible Absorption Cross Sections of Nitrous Acid, *J. Geophys. Res.*, 2000, **105**, 14585–14592.

54 TUV, Quick TUV Calculator, NCAR Earth System Laboratory, Atmospheric chemistry Division, 2015, http://cprm.acd.ucar.edu/Models/TUV/Interactive_TUV/.

55 J. Heland, J. Kleffmann, R. Kurtenbach and P. Wiesen, A New Instrument to Measure Gaseous Nitrous Acid (HONO) in the Atmosphere, *Environ. Sci. Technol.*, 2001, **35**, 3207–3212.

56 G. Villena, I. Bejan, R. Kurtenbach, P. Wiesen and J. Kleffmann, Development of a new Long Path Absorption Photometer (LOPAP) Instrument for the Sensitive Detection of NO_2 in the Atmosphere, *Atmos. Meas. Tech.*, 2011, **4**, 1663–1676.

57 C. Hak, I. Pundt, S. Trick, C. Kern, U. Platt, J. Dommen, C. Ordóñez, A. S. H. Prévôt, W. Junkermann, C. Astorga-Lloréns, B. R. Larsen, J. Mellqvist, A. Strandberg, Y. Yu, B. Galle, J. Kleffmann, J. C. Lörzer, G. O. Braathen and R. Volkamer, Intercomparison of Four Different *In situ* Techniques For Ambient Formaldehyde Measurements in Urban Air, *Atmos. Chem. Phys.*, 2005, **5**, 2881–2900.

58 J. Kleffmann, T. Benter and P. Wiesen, Heterogeneous Reaction of Nitric Acid with Nitric Oxide on Glass Surfaces under Simulated Atmospheric Conditions, *J. Phys. Chem. A*, 2004, **108**, 5793–5799.

Open Access Article. Published on 09 marzo 2016. Downloaded on 30/09/2025 1:16:36 a.m..
This article is licensed under a Creative Commons Attribution 3.0 Unported Licence.

59 A. L. Goodman, E. T. Bernard and V. H. Grassian, Spectroscopic Study of Nitric Acid and Water Adsorption on Oxide Particles: Enhanced Nitric Acid Uptake Kinetics in the Presence of Adsorbed Water, *J. Phys. Chem. A*, 2001, **105**, 6443–6457.

60 J. J. Jankowski, D. J. Kieber and K. Mopper, Nitrate and Nitrite Ultraviolet Actinometers, *Photochem. Photobiol.*, 1999, **70**(3), 319–328.

61 B. J. Finlayson-Pitts, L. M. Wingen, A. L. Sumner, D. Syomin and K. A. Ramazan, The Heterogeneous Hydrolysis of NO_2 in Laboratory Systems and in Outdoor and Indoor Atmospheres: An Integrated Mechanism, *Phys. Chem. Chem. Phys.*, 2003, **5**, 223–242.

62 R. J. Gustafsson, G. Kyriakou and R. M. Lambert, The Molecular Mechanism of Tropospheric Nitrous Acid Production on Mineral Dust Surfaces, *ChemPhysChem*, 2008, **9**, 1390–1393.

63 M. A. Kamboures, J. D. Raff, Y. Miller, L. F. Phillips, B. J. Finlayson-Pitts and R. B. Gerber, Complexes of HNO_3 and NO_3^- with NO_2 and N_2O_4, and their Potential Role in Atmospheric HONO formation, *Phys. Chem. Chem. Phys.*, 2008, **10**, 6019–6032.

64 L. Zhu, M. Sangwan, L. Huang, J. Du and L. T. Chu, Photolysis of Nitric Acid at 308 nm in the Absence and in the Presence of Water Vapor, *J. Phys. Chem. A*, 2015, **119**, 4907–4914.

65 H.-W. Jacobi and B. Hilker, A Mechanism for the Photochemical Transformation of Nitrate in Snow, *J. Photochem. Photobiol., A*, 2007, **185**, 371–382.

66 N. K. Scharko, A. E. Berke and J. D. Raff, Release of Nitrous Acid and Nitrogen Dioxide from Nitrate Photolysis in Acidic Aqueous Solutions, *Environ. Sci. Technol.*, 2014, **48**, 11991–12001.

67 E. S. N. Cotter, A. E. Jones, E. W. Wolff and S. J.-B. Bauguitte, What Controls Photochemical NO and NO_2 Production from Antarctic Snow? Laboratory Investigation Assessing the Wavelength and Temperature Dependence, *J. Geophys. Res.*, 2003, **108**(D4), 4147.

68 J. M. Tadić, Comment on ''308 nm Photolysis of Nitric Acid in the Gas Phase, on Aluminum Surfaces, and on Ice Films'', *J. Phys. Chem. A*, 2012, **116**, 10463–10464.

69 S. R. Handley, D. Clifford and D. J. Donaldson, Photochemical Loss of Nitric Acid on Organic Films: A Possible Recycling Mechanism for NO_x, *Environ. Sci. Technol.*, 2007, **41**, 3898–3903.

70 R. Ammar, M. E. Monge, C. George and B. D'Anna, Photoenhanced NO_2 Loss on Simulated Urban Grime, *ChemPhysChem*, 2010, **11**, 3956–3961.

71 A. M. Baergen and D. J. Donaldson, Photochemical Renoxification of Nitric Acid on Real urban Grime, *Environ. Sci. Technol.*, 2013, **47**, 815–820.

72 D. Cazoir, M. Brigante, R. Ammar, B. D'Anna and C. George, Heterogeneous Photochemistry of Gaseous NO_2 on Solid Fluoranthene Films: A Source of Gaseous Nitrous Acid (HONO) in the Urban Environment, *J. Photochem. Photobiol., A*, 2014, **273**, 23–28.